Inorganic Chemistry

Article

pubs.acs.org/IC

Garnet-to-Perovskite Transition in $Gd_3Sc_2Ga_3O_{12}$ at High Pressure and High Temperature

Chuanlong Lin,[†] Jing Liu,*[,†] Jung-Fu Lin,[‡] Xiaodong Li,[†] Yanchun Li,[†] Qingli Zhang,[§] Lun Xiong,[†] and Rui Li[†]

[†]Beijing Synchrotron Radiation Facility (BSRF), Institute of High Energy Physics, Chinese Academy of Sciences, Beijing 100049, China

[‡]Department of Geological Sciences, Jackson School of Geosciences, The University of Texas at Austin, Austin, Texas 78712, United States

[§]Anhui Institute of Optics and Fine Mechanics, Chinese Academy of Sciences, Hefei 230031, China

ABSTRACT: The structural phase transition of gadolinium−scandium−gallium garnet ($Gd_3Sc_2Ga_3O_{12}$, GSGG) has been studied at high pressure and high temperature using the synchrotron X-ray diffraction technique in a laser-heated diamond anvil cell. The GSGG garnet transformed to an orthorhombic perovskite structure at approximately 24 GPa after laser heating to 1500−2000 K. The garnet-to-perovskite phase transition is associated with an ∼8% volume reduction and an increase in the coordination number of the Ga^{3+} or Sc^{3+} ion. The orthorhombic perovskite GSGG has bulk modulus B_0 = 194(15) GPa with B_0' = 5.3(8), exhibiting slightly less compression than the cubic garnet structure of GSGG with B_0 = 157(15) GPa and B_0' = 6.5(10). Upon compression at room temperature, the cubic GSGG garnet became amorphous at ∼65 GPa. Coupled with the amorphous-to-perovskite phase transition in $Y_3Fe_5O_{12}$ and $Gd_3Ga_5O_{12}$ at high-pressure−temperature conditions, we conclude that amorphization should represent a new thermodynamic state resulting from hindrance of the garnet-to-perovskite phase transition, whereas the garnet-to-amorphous transition in rare-earth garnets should be kinetically hindered at room temperature.

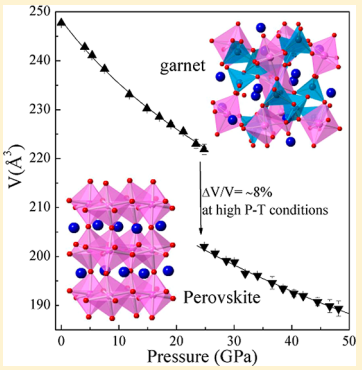

INTRODUCTION

Garnet crystals have the general formula $A_3B_2C_3O_{12}$ with the cubic space group *Ia*3*d* and eight formula units in the unit cell, where A, B, and C denote the dodecahedral, octahedral, and tetrahedral sites in the lattice, respectively. In rare-earth garnets, the A site is occupied by the rare-earth cation, while the B and C sites are occupied by Al^{3+}, Ga^{3+}, Sc^{3+}, or Fe^{3+} cations. It is well-known that the dopant rare-earth garnets exhibit fascinating optical luminescent properties and have been used as a host laser material.[1−7] Additionally, the rare-earth garnets can be used as new optical pressure sensors.[2,8−14]

The pressure-induced crystalline-to-amorphous transformation in the solid state has been the focus of intense study since amorphization of ice water was observed at 1 GPa and 77 K[15] and has been identified in many materials.[16−20] Previous experiments have shown that some of the rare-earth garnets become amorphous upon compression at room temperature. $Gd_3Ga_5O_{12}$ (GGG), $Gd_3Sc_2Ga_3O_{12}$ (GSGG), and $Y_3Fe_5O_{12}$ (YIG) become amorphous at 84, 58, and 50 GPa,[21,22] respectively, whereas $Y_3Al_5O_{12}$ (YAG) remains crystalline cubic up to 101 GPa.[21] Hua et al. have indicated that the high-pressure structural stability of these garnets is related to their unit cell volumes and crystal-field strengths.[21] GSGG and YIG, which have larger unit cell volumes, are easier to amorphize than the rare-earth gallium garnet GGG, which has a smaller unit cell.

The high-pressure phase transition of amorphous garnets after heating is a subject of great research interest because the high-pressure phases have recently been observed to exhibit extremely high incompressibilities.[23,24] Specifically, amorphous GGG transforms to a highly incompressible cubic perovskite phase at 88 GPa after laser heating.[24] The new cubic phase is observed to be stiffer than shock-compressed sapphire and diamond above 170 GPa. Additionally, amorphous YIG transforms to an orthorhombic perovskite phase at high-pressure and high-temperature (high-*P*−*T*) conditions.[25] The amorphous-to-perovskite phase transition in rare-earth garnets requires a very high pressure (84 GPa for GGG[24] and 50 GPa for YIG[25]). However, Marezio et al. reported that YIG and YAG garnets decomposed to $3YFeO_3 + Fe_2O_3$ and $3YAlO_3 + Al_2O_3$ at ∼4 GPa and ∼1150 K for YIG and ∼4.4 GPa and 1300 K for YAG,[26] respectively. It is thus necessary to study the structural transition sequence of other garnets such as GSGG at high-*P*−*T* conditions in order to decipher the underlying mechanisms of these transitions.

In this study, we investigated the phase transition of GSGG at high-*P*−*T* conditions using a laser-heating diamond anvil cell and synchrotron X-ray diffraction techniques. We observed that cubic garnet GSGG transforms into a high-pressure perovskite after laser heating rather than a phase mixture of decomposed

Received: October 14, 2012

 © XXXX American Chemical Society dx.doi.org/10.1021/ic302245x | *Inorg. Chem.* XXXX, XXX, XXX−XXX

phases reported for other rare-earth garnet compounds, whereas the high-pressure amorphization was observed to occur at approximately 65 GPa. We use these results to understand the crystal chemistry and phase-transition sequences in the rare-earth system at high-$P-T$ conditions.

EXPERIMENTAL DETAILS

Polycrystalline GSGG (containing approximately 2 atom % for Yb^{3+}) was prepared by the coprecipitation method. The compound was confirmed to be in a cubic garnet structure via X-ray diffraction and Raman scattering analyses.

For the high-pressure X-ray diffraction analysis of GSGG at room temperature, a pair of diamond anvils with 150 μm culet size was used for observation of the pressure-induced amorphization. NaCl was used as the pressure-transmitting medium, and platinum served as the pressure calibrant.[27] In the high-$P-T$ experiments, 300 μm culets were used. The powder sample was mixed with ~8 wt % platinum, which served as a laser absorber. Argon was cryogenically loaded into the sample chamber as both a pressure medium and a thermal insulator. The garnet sample was then compressed to ~24 GPa and laser-heated to 1500−2000 K.

In situ high-pressure angle-dispersive X-ray diffraction experiments were conducted at the 4W2 beamline of the BSRF with a wavelength of 0.6199 Å and a beam size of approximately 26 × 8 μm^2 (full width at half-maximum). X-ray diffraction patterns were collected by an image plate detector (MAR345) and integrated using the *FIT2D* software package.[28] The diffraction patterns were analyzed using the *GSAS* program.[29]

RESULTS AND DISCUSSION

GSGG crystallizes in a cubic structure with space group $Ia3d$ at ambient conditions. Rietveld refinements of the X-ray diffraction patterns show a good agreement with the garnet structure at ambient pressure (Figure 1) in which the ionic

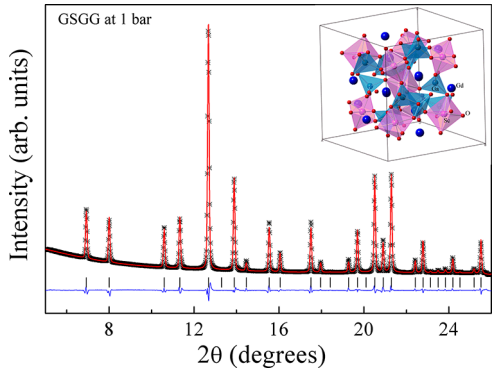

Figure 1. Refined diffraction pattern of GSGG at ambient conditions. The inset shows the corresponding crystal structure of the cubic garnet GSGG.

Gd^{3+}, Sc^{3+}, and Ga^{3+} ions occupy the dodecahedral, octahedral, and tetrahedral sites in the lattice, respectively, forming a three-dimensional network (inset of Figure 1). Each O atom belongs to two dodecahedra, one tetrahedron, and one octahedron. Upon compression at room temperature, the X-ray diffraction peaks of the cubic garnet shift to higher diffraction angles and are broadened (Figure 2). The diffraction peaks collapsed into a broad peak at ~65 GPa, indicating the loss of the long-range order and onset of the amorphous state. This amorphization of GSGG is in agreement with previous reports.[21]

Distinctly different diffraction peaks were observed after GSGG was laser-heated at ~24 GPa (Figure 3), suggesting the occurrence of an intermediate phase change between the garnet

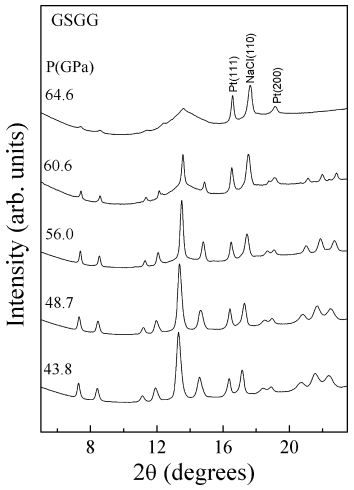

Figure 2. Representative angle-dispersive X-ray diffraction patterns (wavelength λ = 0.6199 Å) of GSGG during compression at room temperature. NaCl was used as the pressure-transmitting medium.

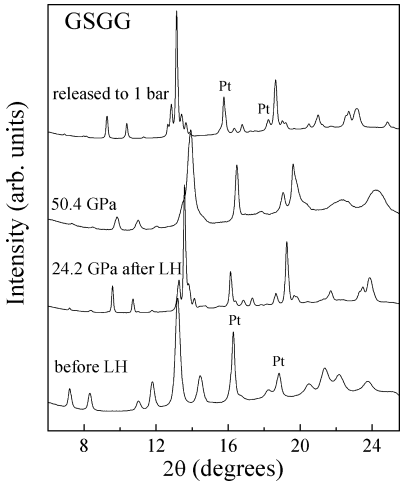

Figure 3. Representative angle-dispersive X-ray diffraction patterns (wavelength λ = 0.6199 Å) of GSGG after laser heating. The diffraction patterns before laser heating are given for comparison.

and amorphous states. When we repeated the laser-heating experiments of the temperature-quenched sample at ~38 GPa, no further phase transition occurred. According to diffraction patterns, small amounts of the garnet phase remained in both laser-heating experiments (Figure 3). The sample was then compressed to ~50 GPa, but there was no obvious change except for the shift of diffraction peaks to higher, broader angles. The diffraction patterns of the intermediate phase can be decompressed to ambient pressures (Figure 3). We also laser-heated the amorphous GSGG at ~65 GPa, but no phase transition was observed. The phase transition of amorphous GSGG at higher-$P-T$ conditions will be the subject of further investigation.

It has been suggested that the rare-earth garnets would undergo a decomposition transformation, $R_3B_2C_3O_{12} \rightarrow 3RCO_3 + B_2O_3$, at high-$P-T$ conditions.[26] Our diffraction patterns of GSGG after laser heating and then temperature quenching at 24−38 GPa do not show diffraction peaks of Sc_2O_3 or Ga_2O_3,[30,31] ruling out the occurrence of the decomposed mixtures of $3GdGaO_3 + Sc_2O_3$. Actually, these diffraction patterns of GSGG are similar to the orthorhombic

dx.doi.org/10.1021/ic302245x | *Inorg. Chem.* XXXX, XXX, XXX−XXX

perovskite structure of $SmNiO_3$ and $GdMnO_3$.[32,33] Using the program *Dicvol*,[34] the new diffraction peaks of GSGG can be well indexed into an orthorhombic phase with the space group *Pbnm*. The unit cell parameters of the high-pressure phase have the relationship $a \approx b \approx c/2^{1/2}$, consistent with those of the orthorhombic perovskite ABO_3. On the basis of these results, we propose that the high-pressure phase of GSGG belongs to the orthorhombic perovskite structure (ABO_3). We note that the garnet-to-orthorhombic phase transition has also been observed in YIG and silicate garnets such as grossular ($Ca_3Al_2Si_3O_{12}$) and pyrope ($Mg_3Al_2Si_3O_{12}$) at high-P–T conditions.[25,35−40]

Figure 4 shows that the observed diffraction patterns of the high-pressure phase of GSGG are well fitted with the model of

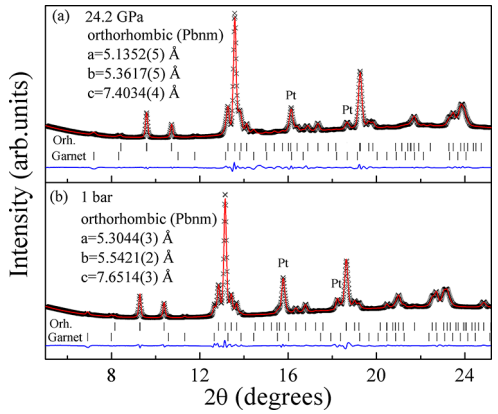

Figure 4. Refined diffraction patterns of the orthorhombic perovskite GSGG. The diffraction pattern at 24.2 GPa was obtained after laser heating of the cubic garnet GSGG. The pattern at 1 bar was quenchable. Symbols: observed patterns. Red solid line: calculated patterns. Blue solid line: differences in the observed and calculated patterns. Black vertical ticks: diffraction positions of the orthorhombic (top) and garnet (bottom) phases.

the orthorhombic perovskite structure (ABO_3) at 24.2 GPa and 1 bar, respectively. On the basis of the stoichiometry and structural transition models proposed here, the orthorhombic perovskite phase of GSGG should have the chemical formula $(Gd_{0.75}Sc_{0.25})(Sc_{0.25}Ga_{0.75})O_3$. The unit cell parameters of the orthorhombic structure were determined to be a = 5.1352(5) Å, b = 5.3617(5) Å, and c = 7.4034(4) Å with V = 203.84(5) Å^3 at 24.2 GPa. The garnet-to-perovskite transition is associated with ∼8% volume reduction at 24.2 GPa. Taking the compressional behavior of the starting cubic phase into account, four formula units (Z = 4) in the unit cell are reasonably assigned for the new orthorhombic phase. In the perovskite structure, the Gd^{3+} and Sc^{3+} cations should occupy the dodecahedral site, while the remaining Sc^{3+} and Ga^{3+} cations stay in the octahedral site according to the size of their ionic radii. This indicates that the perovskite structure of the high-pressure GSGG is a nonequivalent A-site tilt system. Therefore, the garnet-to-perovskite phase transition is associated with an increase of the coordination number from 4 to 6 for Ga^{3+} or from 6 to 12 for Sc^{3+}.

Mao et al. reported that the amorphous GGG transformed to the cubic perovskite structure at 88 GPa upon laser heating up to 1500 K.[24] The volume of the unit cell for the cubic perovskite phase GGG is 336.1(1) Å^3 at 92 GPa with eight chemical formulas $(Gd_{0.75}Ga_{0.25})GaO_3$ or two formulas $Gd_3Ga_5O_{12}$ in the unit cell, twice as large as the orthorhombic perovskite GSGG. To the best of our knowledge, the cubic perovskite structure should have space group $Pm\bar{3}m$ or $I\bar{3}m$. However, the indices *hkl* of the cubic perovskite GGG are not consistent with the reflection conditions of the space group $Pm\bar{3}m$ or $Im\bar{3}$. Actually, the diffraction pattern of the orthorhombic GSGG shows some similarity with that of the cubic perovskite GGG. Additionally, we found that the high-pressure phase GGG can also be indexed into the orthorhombic perovskite structure according to the peak positions listed in Table 1 of Mao et al.[24] These indicate that the garnet GSGG may undergo a phase transition similar to amorphous GGG at high-P–T conditions.

Pressure-induced amorphization may be related to chemical decomposition. In the amorphization process, the parent crystal decomposes into corresponding oxide mixtures. This is favored if the daughter compounds occupy less volume than the parent crystal.[41] For GSGG, the mixture phase of $3GdGaO_3 + Sc_2O_3$ is ∼9.6% denser than the parent garnet phase at ambient pressure. On the basis of this information, the garnet GSGG should decompose into the more densely packed crystalline daughter compounds during the pressure-induced amorphization process. However, we failed to obtain the mixture of $3GdGaO_3 + Sc_2O_3$ during laser heating of the amorphous sample GSGG. Instead, the garnet GSGG transformed to the orthorhombic phase at high-P–T conditions rather than decomposing. This indicates that the orthorhombic phase is more stable than the mixed phase for GSGG. Combined with the amorphous-to-perovskite phase transition in YIG and GGG at high-P–T conditions,[24,25] it seems that the pressure-induced garnet-to-amorphous transition in rare-earth garnets may be kinetically hindered at room temperature. Amorphization should thus be considered a new thermodynamic state resulting from the hindrance of a crystal-to-crystal phase transition.

Figure 5 shows the pressure dependences of the unit cell volumes for garnet GSGG and perovskite GSGG. The

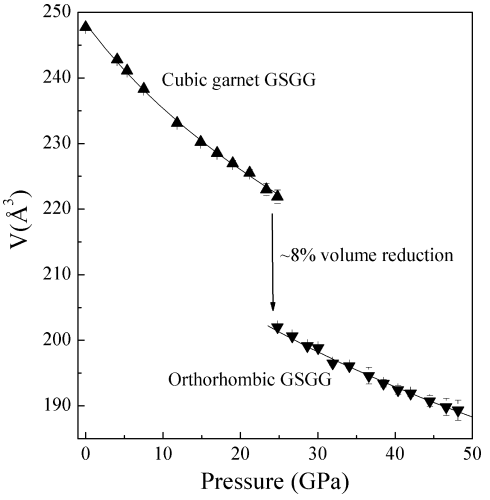

Figure 5. Experimental P–V data of the garnet and high-pressure orthorhombic perovskite phases GSGG. The solid line is the fit with the Birch–Murnaghan EOS for the P–V data.

pressure–volume (P–V) data is fitted to a third-order Birch–Murnaghan equation of state (EOS),[42] which yields the bulk modulus (B_0) with a pressure derivative of the bulk modulus (B_0'). For garnet GSGG, fitting the P–V data yields bulk modulus B_0 = 157(15) GPa with B_0' = 6.5(10) and V_0 =

dx.doi.org/10.1021/ic302245x | Inorg. Chem. XXXX, XXX, XXX–XXX

248.3(8) Å^3, where V_0 is the unit cell volume at ambient pressure. When B_0' is fixed to 4.0, the bulk modulus B_0 obtained is 195(5) GPa with V_0 = 246.8(5) Å^3. The bulk modulus of the orthorhombic perovskite GSGG is 194(15) GPa with V_0 = 222.2(7) Å^3 and B_0' = 5.3(8) or 223(4) GPa with V_0 = 221.1(4) Å^3 and B_0' = 4 (fixed). The orthorhombic perovskite GSGG is slightly less compressible than the cubic garnet GSGG. However, the bulk modulus of the orthorhombic perovskite GSGG is obviously smaller than the value [373(5) GPa] reported for the high-pressure cubic perovskite GGG.

■ CONCLUSION

In conclusion, we have observed a pressure-induced garnet-to-amorphous transition in compressed GSGG at ∼65 GPa. Upon laser heating, the garnet structure of GSGG transforms to an orthorhombic perovskite structure at ∼24 GPa rather than decompositing at high-P−T conditions as reported earlier. The metastable orthorhombic structure can be quenched. The garnet-to-perovskite phase transition is associated with an ∼8% volume reduction and an increase of the coordination number of the Ga^{3+} or Sc^{3+} ion. The high-pressure orthorhombic structure has slightly higher compressibility compared to the cubic garnet phase.

■ AUTHOR INFORMATION

Corresponding Author

*E-mail: liuj@ihep.ac.cn.

Notes

The authors declare no competing financial interest.

■ ACKNOWLEDGMENTS

The authors are grateful to N. Seymour, The University of Texas at Austin, for a careful reading of the manuscript. Financial support from the National Natural Science Foundation of China (Grant 11079040) and the National Basic Research Program of China (Grant 2011CB808200) is gratefully acknowledged. The experimental work was performed at the 4W2 beamline of BSRF, which was supported by the Chinese Academy of Sciences (Grants KJCX2-SW-N20 and KJCX2-SW-N03). Work at The University of Texas at Austin was supported by Energy Frontier Research in Extreme Environments (EFree) and the Carnegie/DOE Alliance Center (CDAC). Work for the sample preparation was supported by the National Natural Science Foundation of China (Grants 90922003 and 51172236).

■ REFERENCES

(1) Gruber, J. B.; Hills, M. E.; Morrison, C. A.; Turner, G. A.; Kokta, M. R. *Phys. Rev. B* **1988**, *37*, 8564.
(2) Hommerich, U.; Bray, K. L. *Phys. Rev. B* **1995**, *51*, 12133.
(3) Antic-Fidancev, E.; Holsa, J.; Lastusaari, M.; Lupei, A. *Phys. Rev. B* **2001**, *64*, 195108.
(4) Heer, S.; Wermuth, M.; Kramer, K.; Gudel, H. U. *Phys. Rev. B* **2002**, *65*, 125112.
(5) Nikl, M.; Novoselov, A.; Mihokova, E.; Polak, K.; Dusek, M.; McClune, B.; Yoshikawa, A.; Fukuda, T.; et al. *J. Phys.: Condens. Matter* **2005**, *17*, 3367.
(6) Zhu, N.; Li, Y.; Yu, X. *Mater. Lett.* **2008**, *62*, 2355.
(7) Zorenko, Y.; Zorenko, T.; Vistovskyy, V.; Grinberg, M.; Lukasiewicz, T. *Opt. Mater.* **2009**, *31*, 1835.
(8) Liu, J.; Vohra, Y. K. *Solid State Commun.* **1993**, *88*, 417.
(9) Liu, J.; Vohra, Y. K. *Appl. Phys. Lett.* **1994**, *64*, 3386.
(10) Liu, J.; Vohra, Y. K. *J. Appl. Phys.* **1996**, *79*, 7978.
(11) Kobyakov, S.; Kamińska, A.; Suchocki, A.; Galanciak, D.; Malinowski, M. *Appl. Phys. Lett.* **2006**, *88*, 234102.
(12) Shen, Y. R.; Bray, K. L. *Phys. Rev. B* **1997**, *56*, 10882.
(13) Kamińska, A.; Biernacki, S.; Kobyakov, S.; Suchocki, A.; Boulon, G.; Ramirez, M. O.; Bausa, L. *Phys. Rev. B* **2007**, *75*, 174111.
(14) Galanciak, D.; Grinberg, M.; Gryk, W.; Kobyakov, S.; Suchocki, A.; Boulon, G.; Brenier, A. *J. Phys.: Condens. Matter* **2005**, *17*, 7185.
(15) Mishima, O.; Calvert, L. D.; Whalley, E. *Nature* **1984**, *310*, 393.
(16) Hemley, R. J.; Jephcoat, A. P.; Mao, H. K.; Ming, L. C.; Manghnani, M. H. *Nature* **1988**, *334*, 52.
(17) Paraguassu, W.; Maczka, M.; Souza, A. G.; Freire, P. T. C.; Mendes, J.; Hanuza, J. *Phys. Rev. B* **2010**, *82*, 174110.
(18) Le Bacq, O.; Machon, D.; Testemale, D.; Pasturel, A. *Phys. Rev. B* **2011**, *83*, 214101.
(19) Gillet, P.; Badro, J.; Varrel, B.; Mcmillan, P. F. *Phys. Rev. B* **1995**, *51*, 11262.
(20) Perottoni, C. A.; da Jornada, J. A. H. *Science* **1998**, *280*, 886.
(21) Hua, H.; Mirov, S.; Vohra, Y. K. *Phys. Rev. B* **1996**, *54*, 6200.
(22) Gavriliuk, A. G.; Struzhkin, V. V.; Lyubutin, I. S.; Eremets, M. I.; Trojan, I. A.; Artemov, V. V. *JETP Lett.* **2006**, *83*, 37.
(23) Mashimo, T.; Chau, R.; Zhang, Y.; Kobayoshi, T.; Sekine, T.; Fukuoka, K.; Syono, Y.; Kodama, M.; Nellis, W. J. *Phys. Rev. Lett.* **2006**, *96*, 105504.
(24) Mao, Z.; Dorfman, S. M.; Shieh, S. R.; Lin, J. F.; Prakapenka, V. B.; Meng, Y.; Duffy, T. S. *Phys. Rev. B* **2011**, *83*, 054114.
(25) Wang, J.; Mao, Z.; Dorfman, S. M.; Prakapenka, V. B.; Duffy, T. S. *Fall Meet. Suppl. EOS Trans. AGU* **2009**, *90*, MR13A.
(26) Marezio, M.; Remeika, J. P.; Jayarama, A. *J. Chem. Phys.* **1966**, *45*, 1821.
(27) Holmes, N. C.; Moriarty, J. A.; Gathers, G. R.; Nellis, W. J. *J. Appl. Phys.* **1989**, *66*, 2962.
(28) HammersleyJ.*Fit2d User Manual*; ESRF: Grenoble, France, 1996
(29) Toby, B. H. *J. Appl. Crystallogr.* **2001**, *34*, 210.
(30) Yusa, H.; Tsuchiya, T.; Sata, N.; Ohishi, Y. *Inorg. Chem.* **2009**, *48*, 7537.
(31) Tsuchiya, T.; Yusa, H.; Tsuchiya, J. *Phys. Rev. B* **2007**, *76*, 174108.
(32) Amboage, M.; Hanfland, M.; Alonso, J. A.; Martinez-Lope, M. J. *J. Phys.: Condens. Matter* **2005**, *17*, S783.
(33) Lin, C. L.; Zhang, Y. F.; Liu, J.; Li, X. D.; Li, Y. C.; Tang, L. Y.; Xiong, L. *J. Phys.: Condens. Matter* **2012**, *24*, 115402.
(34) Boultif, A.; Louer, D. *J. Appl. Crystallogr.* **2004**, *37*, 724.
(35) Yusa, H.; Yagi, T.; Shimobayashi, N. *Phys. Earth Planet. Inter.* **1995**, *92*, 25.
(36) Greaux, S.; Nishiyama, N.; Kono, Y.; Gautron, L.; Ohfuji, H.; Kunimoto, T.; Menguy, N.; Irifune, T. *Phys. Earth Planet. Inter.* **2011**, *185*, 89.
(37) Irifune, T.; Koizumi, T.; Ando, J. I. *Phys. Earth Planet. Inter.* **1996**, *96*, 147.
(38) Ito, E.; Kubo, A.; Katsura, T.; Akaogi, M.; Fujita, T. *Geophys. Res. Lett.* **1998**, *25*, 821.
(39) Walter, M. J.; Kubo, A.; Yoshino, T.; Brodholt, J.; Koga, K. T.; Ohishi, Y. *Earth Planet. Sci. Lett.* **2004**, *222*, 501.
(40) Tateno, S.; Hirose, K.; Sata, N.; Ohishi, Y. *Geophys. Res. Lett.* **2005**, *32*, L15306.
(41) Arora, A. K. *Solid State Commun.* **2000**, *115*, 665.
(42) Birch, F. *J. Geophys. Res.* **1978**, *83*, 1257.